Simulation of Quantum Electronic Devices Using the Recursive Green's Function Method

Qin Li and D. K. Ferry
Center for Solid State Electronics Research
Arizona State University, Tempe, AZ 85287

Abstract

The recursive Green's function method has been implemented to study the transport properties of submicron electronic devices. We have performed a self-consistent calculation of electron transport in a narrow wire. We consider the local electrostatic potential distribution in a quantum wire and take the Coulomb interaction into account in the Hartree approximation. The results for a narrow wire with a smooth potential barrier show that there is Friedel oscillation in the electron density near the gate. Conductance steps are preserved when the Hartree potential is explicitly taken into account, although the steps are shifted towards higher gate voltages. We also study the magneto-transport properties, particularly the interplay between the magnetic field and a periodic potential. There is rich structure in both the density of states and the conductance, reflecting the devil's staircase energy spectrum of such systems.

I. Self-consistent Calculation of the Quantized Conductance

Advances in microdevice fabrication has created both the possibility and the necessity to study electronic transport in the ballistic regime, in which the sample size is smaller than the elastic and inelastic lengths. One remarkable discovery in ballistic transport is quantized conductance steps that are integer multiples of e^2/h in quantum point contacts, i.e. split-gate constrictions [1,2]. These conductance steps can be explained as being due to the perfect transmission of the transverse modes below the Fermi energy of the constriction. Subsequent theoretical investigations have revealed that the sharpness of the steps depends exponentially on the smoothness of the ends of the constriction [3-6]. In a recent paper [7], we have shown that these conductance steps should be observable in narrow wires (e.g. 100 nm wide) with a smooth potential barrier, and the width of the step is proportional to the energy gap between the thresholds of neighboring lateral modes.

We consider the local electrostatic potential distribution in a quantum wire. The Coulomb interaction is taken into account in the Hartree approximation. We use the recursive Green's function method [8-10] in which the system is represented by a tight-binding Hamiltonian. The Green's function is calculated through repeated use of the Dyson equation and a careful choice of the unperturbed and the perturbing Hamiltonians. At temperature $T = 0$ K, the electron density is calculated by integrating the density of states (the imaginary part of the Green's function) from the lower band edge to the Fermi energy. It is straightforward to extend the calculation to nonzero temperature by including the Fermi-Dirac distribution function in the integral and let the upper limit of the integral go to infinity. A more relevant quantity is the excess electron density which is defined as the difference between the electron density and the background positive charge density. After evaluating the excess charge density, the Hartree potential is calculated and included as a part of the site energy. Self-consistency is achieved by iteration of the entire procedure. Finally, the conductance is computed using the Kubo formula.

To illustrate the usefulness of the method described, we consider a simple example, i.e. a narrow wire with a smooth potential barrier. We start with the Green's function of a semi-infinite chain. The system is built up first starting from the right end and the Green's function on each step is stored. Next the same system is constructed from the left end and the resulting Green's function

is joined with the appropriate pieces from the right end to get the full Green's function for the entire system on each slice. The process is repeated for all energies below the Fermi energy and this takes most of the CPU time. When the integral calculating the excess charge density is discretized, the energy step should be taken comparable to or smaller than the broadening δ of the energy levels. After obtaining the excess charge density, the Hartree potential can be calculated easily. To eliminate the undesirable effect of a sizable, although decreasing, electric field in the leads screening must be taken into account and, as is well known [11], this leads to an electrostatic potential which falls off asymptotically as r^{-3}. In the numerical calculation one can simply limit the sum to range only over sites that are within a certain range of the potential barrier. The range is determined to be twice the length of the gate so that the potential near the gate, where the excess charge density significantly differs from zero, remains unchanged within the numerical accuracy, while the charge neutrality is maintained in the leads. The numerical result for the excess charge density is shown in Fig. 1 and it is interesting to note that, in addition to the usual charge depletion underneath the gate, there are Friedel oscillations [12] in the charge density which decay gradually as one moves away from the depletion region. The convergence is determined by plotting the excess charge density as in Fig. 1 for a number of successive iterations and it is found that satisfactory convergence is achieved after 5 iterations. The numerical accuracy after 5 iterations is typically better than 5% at the peaks and valleys of the Friedel oscillations, and it can be improved simply with more iterations. It is also found that there is little change when the energy step is changed from 0.005 to 0.001 for $\delta = 0.005$, so a smaller energy step is not necessary.

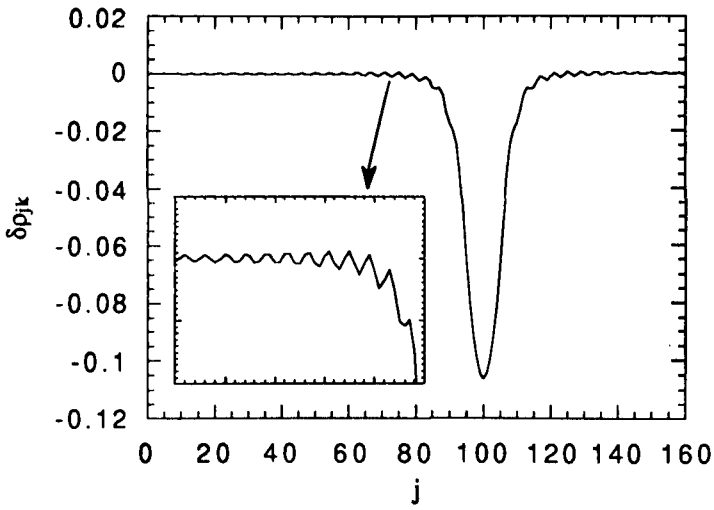

Fig. 1. The excess electron density along the center of the wire. In addition to the usual charge depletion underneath the gate there are Friedel oscillations at the two sides of the depletion region. The system size is 200 x 6 sites. Good convergence is achieved with five iterations. The energy step is 0.001 and δ= 0.005.

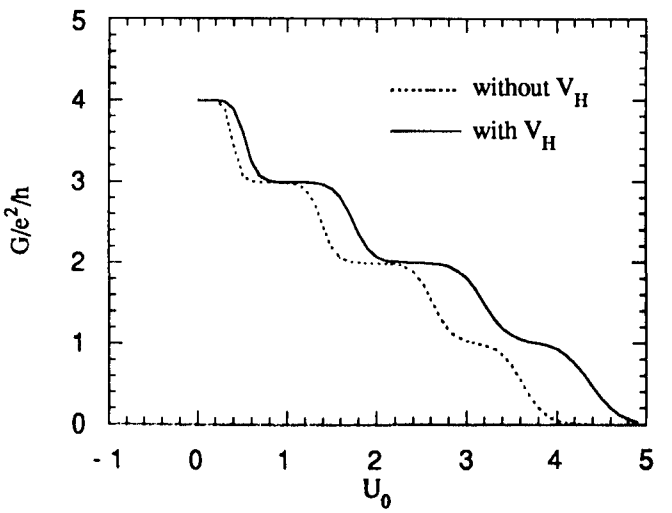

Fig. 2. The conductance as a function of the barrier height with and without the Hartree potential. G is in units e^2/h and the barrier hight U_0 is measured in units of the site-coupling energy.

With the Green's function in hand, we can calculate the conductance directly using the Kubo formula [13] and the result is shown in Fig. 2. There are several interesting features worth noting. First, we note that the same conductance steps without the Hartree potential are obtained in Ref. 7 using the Landauer formula approach, and the agreement of the present result with that of Ref. 7 clearly demonstrates the equivalence of the Landauer formula and the Kubo formula. Second the conductance steps are not perturbed by the electron-electron interaction, but merely shift towards higher gate potentials. This is expected as the self-consistent potential tends to reduce the applied voltage. There is no qualitative difference between the conductance steps with the Hartree potential and those without the Hartree potential.

II. The Interplay of the Magnetic Field and the Periodic Lattice

The motion of electron in a magnetic field and a periodic potential is an intriguing problem and has long been a subject of much research effort [14-20]. Particularly in both the strong periodic potential, weak magnetic field and the strong magnetic field, weak periodic potential cases, the energy bands and/or the magnetic Landau levels are split to give rise to an intricate devil's staircase energy spectrum [15,16]. Although it requires a prohibitively large magnetic field ($\sim 10^4$ T) to get a simple fraction of a flux quantum through a crystal unit cell, advances in nanolithography have made it possible to fabricate lateral surface superlattice type devices [18,19], in which the lattice periodicity is about 160 nm. Thus, it is now possible to explore the intricate energy spectrum experimentally [20]. It has also been shown that a quantized Hall conductance is associated with each energy subband as a topological invariant [17].

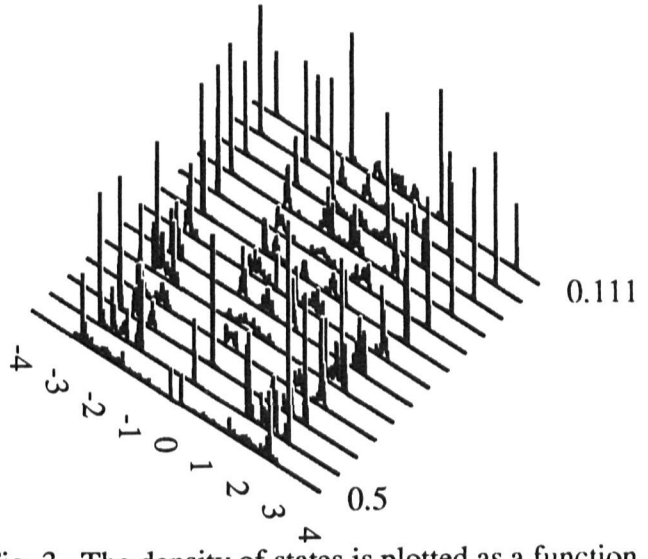

Fig. 3. The density of states is plotted as a function of energy for several simple fractional numbers of flux quantum per unit cell: 1/2, 4/9, 3/7, 2/5, 1/3, 2/7, 1/4, 2/9, 1/5, 1/6, 1/7, 1/8, 1/9.

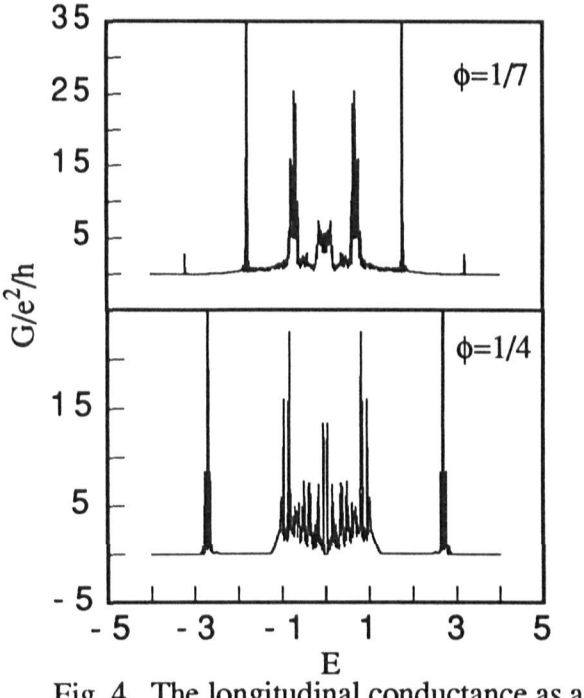

Fig. 4. The longitudinal conductance as a function of energy for 1/4 and 1/7 flux quantum per unit cell.

It is rather natural to use the recursive Green's function method to study this problem. Periodicity is built-in into the Hamiltonian and the magnetic field is easily incorporated. Disorder can also be included by a randomly distributed the site-energy. In Fig. 3, we show the calculated density of states for several fractions from 1/9 to 1/2 flux quantum per unit cell. The energy band

is split into q bands, where q is the denominator of the fractional number of flux quantum per unit cell. For even q, the middle two bands touch at the center (E = 0) and appear as one band, but with a vanishing density of states at the center. The density of states plot can be viewed as a 3D presentation of Hofstadter's "Butterfly" energy spectrum [15]. The longitudinal conductance is shown in Fig. 4 for 1/4 and 1/7 flux quantum per unit cell. When the Fermi energy lies in the subbands the conductance is non zero and fluctuates rapidly with the Fermi energy.

Acknowledgment

The authors wish to thank Y. Takagaki, K. Yano and J. R. Zhou for helpful discussions. This work is supported by the Office of Naval Research.

References

1. B. J. van Wees, H. van Houten, C. W. J. Beenakker, J. G. Williamson, L. P. Kouwenhoven, D. van der Marel, and C. T. Foxon, *Phys. Rev. Lett.* **60**, 848 (1988).
2. D. A. Wharam, T. J. Thorton, R. Newbury, M. Pepper, H. Ahmed, J. E. F. Frost, D. G. Hasko, D. C. Peacock, D. A. Richie, and G. A. C. Jones, *J. Phys. C* **21**, L209 (1988).
3. L. I. Glazman, G. B. Lesovik, D. E. Khmel'nitskii, and R. I. Shekter, *Pis'ma Zh. Eksp. Teor. Fiz.* **48**, 218 (1988) [*JETP Lett.* **48**, 238 (1988)].
4. A. Szafer and A. D. Stone, *Phys. Rev. Lett.* **62**, 300 (1989).
5. A. Yacoby and Y. Imry, *Phys. Rev. B* **41**, 5341 (1990).
6. M. Büttiker, *Phys. Rev. B* **41**, 7906 (1990).
7. Q. Li and D. K. Ferry, *Superlattices and Microstructures* **11**, 245 (1992).
8. D. J. Thouless and S. Kirkpatrick, *J. Phys. C* **14**, 235 (1981).
9. D. S. Fisher and P. A. Lee, *Phys. Rev. B* **23**, 6851 (1981).
10. A. MacKinnon, *Z. Phys. B* **59**, 385 (1985).
11. T. Ando, A. B. Fowler, and F. Stern, *Rev. Mod. Phys.* **54**, 437 (1982).
12. J. Friedel, *Phil. Mag.* **43**, 153 (1952).
13. P. A. Lee and D. S. Fisher, *Phys. Rev. Lett.* **47**, 882 (1981).
14. P. G. Harper, *Proc. Phys. Soc. (London) A* **68**, 874 (1955).
15. D. Hofstadter, *Phys. Rev. B* **14**, 2239 (1976).
16. M. Ya. Azbel, *J. Exptl. Theoret. Phys.* **46**, 929 (1964) [*Sov. Phys. JEPT* **19**, 634 (1964)].
17. D. J. Thouless, M. Kohomoto, M. P. Nightingale, and M. den Nijs, *Phys. Rev. Lett.* **49**, 405 (1982).
18. D. K. Ferry, G. Bernstein, R. Puechner, J. Ma, A. M. Kriman, R. Mezenner, W.-P. Liu, G. N. Maracas, and R. Chamberlin, in *High Magnetic Fields in Semiconductor Physics II*, Ed. by G. Landwehr (Springer-Verlag, Berlin, 1989).
19. J. Ma, R. A. Puechner, W.-P. Liu, A. M. Kriman, G. N. Maracas, and D. K. Ferry, *Surf. Sci.* **229**, 341 (1990).
20. R. R. Gerhardts, D. Weiss, and U. Wulf, *Phys. Rev. B* **43**, 5192 (1991).